Behaviour of a small Wells turbine under randomly varying oscillating flow

S. M. Camporeale[1], P. Filianoti[2]

[1] "Politecnico di Bari" University –DIMeG Department
E-mail: camporeale@poliba.it
[2] University Mediterranean of Reggio Calabria – Okeanòs Laboratory
e-mail: filianoti@unirc.it

Abstract

A monoplane Wells turbine was tested during the experiments conducted at sea on a small scale model of a REWEC (Resonant Wave Energy Converter) breakwater. Tests aimed at analyzing the behaviour of the turbine subjected to randomly varying oscillating air flow, variable according to the intensity and spectral characteristics of the sea. During the experimental campaign, 261 records (sea states) were acquired in order to characterize the behaviour of both the plant and turbine. Thanks to the measurement techniques ad hoc developed for tests at sea and described in a companion paper, it was possible to determine the values of torque coefficient T^* and pressure coefficient Δp^* as a function of the flow coefficient, ϕ. Because during each sea state lasting five minutes, data on dozens of cycles of oscillation were recorded, it was possible to perform a statistical analysis of all the available data, with regard to the sign of ϕ and of its derivative. The results were classified by maximum oscillation amplitude and peak frequency of the spectrum. The paper presents the results of the statistical analysis carried out by highlighting the effects on the stall condition at high values of flow coefficient and on the hysteresis between the phases in which the flow rate is growing and those where the flow rate is decreasing. Finally, the influence of the spectral components at higher frequencies on the hysteresis phenomenon was highlighted.

Keywords: Wells turbine, hysteresis, characteristic curves, flow pattern.

1 Introduction

In the last two decades, within the research interest in renewable energy, efforts have been devoted to exploit the benefits of sea wave energy by means of different kinds of devices [1]. One of the most interesting research field is focused on Oscillating Water Column (OWC) devices (see, e.g., Falcão [2]) that are fixed plants and hence easier to be built and maintained.

The energy of the oscillating air flow produced inside OWCs can be effectively converted into an unidirectional rotational motion by the self-rectifying Wells turbine. In order to improve the energy conversion process, the turbine should have good efficiency for a wide range of flow-rate [3–5]. To this purpose, analyses of the flow through the Wells turbine have been carried out by means of experimental [6–8], analytical [9, 10] and CFD simulations [11–14]. In particular, three-dimensional simulations were carried out by: Thakker et al. [11] in order to investigate the influence of blade profile; Kim et al. [12] in order to study influence of the blade sweep; Dhanasekaran and Govardhan [13] in order to investigate the characteristics of a Wells turbine with NACA0021 constant chord blades; and Torresi et al. [14] to evaluate the tip clearance effects.

The most of the experimental and numerical investigations have been carried out under steady unidirectional flow conditions, assuming that, in consideration of the low sea wave frequencies, a quasi-steady approach can be employed to analyse the turbine performance. Recently, a few works have shown that the quasi-steady approach is not completely representative of the actual working conditions of the turbine at sea, where the flow is bidirectional and randomly variable.

Kinoue et al. [15] - [17], by means of unsteady CFD simulations observed hysteretic effects under oscillating flow conditions, especially when the oscillating amplitude become large. Thakker and Abdulhadi [18] realised a test rig able to produce a bidirectional air flow through a 0.6 m diameter Wells turbine. They compared the average turbine efficiency obtained from experiments with that evaluated from steady-state measurements. This comparison showed that the mean calculated efficiency was in good agreement with the experimental measured mean efficiency, especially at low flow coefficient. Thakker and Abdulhadi provided also experimental results on

© Proceedings of the 8th European Wave and Tidal Energy Conference, Uppsala, Sweden, 2009

instantaneous turbine torque and efficiency: however, they did not identify unsteady fluid-dynamic effects, produced on the measured torque, by the variation of momentum of inertia of the rotating parts, because of fluctuations in the rotational speed.

As shown in the companion paper [19], Filianoti and Camporeale tested a small Wells turbine in the course of small scale field experiment on a REWEC3 breakwater [20]. The plant is the 1:10 scale model of a innovative OWC plant, named Resonant Wave Energy Converter (model n. 3), REWEC3, patented by Boccotti ([21]-[24]). This system is essentially a caisson breakwater embodying an OWC with an additional vertical duct, which connects the plant to the sea through a small outer opening. Waves cannot enter the plant, and the oscillations of the water column in the U-duct, constituted by the vertical duct and the plenum chamber, are forced by wave pressure fluctuations acting on the small opening [25] of the vertical duct. The innovative characteristics of this original solution are described by the inventor and his co-workers ([26], [27]).

This experiment, had two main aims:

- to analyse the energy conversion from the fluctuating water flow at the outer opening of the vertical duct to the fluctuating air motion across the turbine;
- to analyse the performance of the Wells turbine under real, randomly varying sea conditions, that are most difficult to reproduce in laboratory.

The Wells turbine was a small monoplane turbine of 0.31 m diameter, without guide vanes. The experiment and the turbine characteristic are summarized in Section 2, while details on the measurement techniques are given in the companion paper [19]. Here some results on the unsteady performance of the turbine are classified and discussed, taking into account:

- the effect on the time period of the incident waves
- the effects of the amplitude of the fluctuation of the flow coefficient
- the effect of the power spectrum of the pneumatic power acting on the turbine.

2 Turbine characteristics and driving system

2.1 Description of turbine prototype and measurement instruments

The breakwater built in the natural laboratory of Reggio Calabria was 16.3 m long, and it is realized by nine caissons close to each other. Each caisson consists of three interconnected cells, where air can flow from one cell to another of the same caisson through holes (indicated by *H* in Figure 1). The central caisson is equipped with a small scale prototype of Wells turbine, placed in a duct connected to the central cell of the caisson (see Figure 1) .

A small prototype of a monoplane Wells turbine without guide vanes has been built for this experiment.

The Wells turbine prototype, see Figure 2, designed to be coupled with this breakwater, is characterized by the following parameters: R_{hub} = 101mm, R_{tip} = 155mm, blade chord c = 74mm, number of blades N = 7, constant chord NACA0015 blade profile. Therefore, the hub-to-tip ratio and the solidity are equal to 0.65 and 0.64, respectively. The hub, divided into two parts, is made up of aluminium and comes from a commercial fan. The blades have been produced in composite material reinforced by carbon fibre with suitable attachment in order to fix the blade with a stagger angle of 90 deg. The turbine shaft is overhung in order to avoid the bearings disturbing the incoming flow. The generator and the optical wheel for speed measurements are housed in a inner duct having the same radius of the turbine hub. Both the two ends of this inner ducting, the one facing the curve connecting the air tube with the plenum chamber, and the one facing the diffuser, are streamlined (see Fig. 2) in order to reduce losses due to constriction/expansion of the flow entering/exiting the annular ring at the outside of this duct.

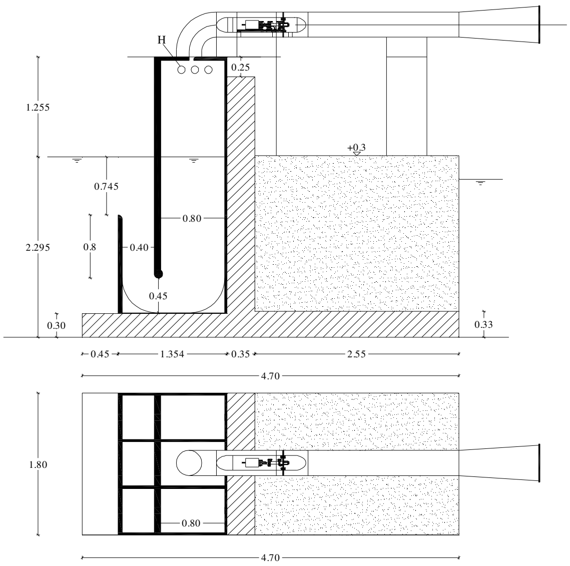

Figure 1 - The central caisson of the absorber breakwater onto which was installed the turbine. [Dimensions are in meters and referred to the m.w.l.]

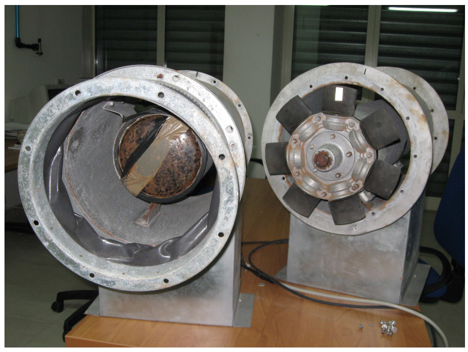

Figure 2 - The small scale model of the Wells turbine off the air tube, recovered after its use at sea.

The turbine shaft is connected to a self ventilated DC motor of permanent magnet type. The DC motor has a double function: 1) it is used as a motor to accelerate the Wells turbine, which is not self-starting; 2) it is used as a dynamo when the turbine speed is sufficiently high and the pneumatic power is enough to enable the turbine to produce power. An electronic power device was purposely designed and realised in order to operate the turbine during the experiment. The device provides the following actions:

(i) to supply current to the electric motor at start-up in order to accelerate the turbine until it reaches the rotational speed sufficient to give a positive torque;

(ii) to act as a variable resistive load able to dissipate the electrical energy produced by the electrical motor when acting as a dynamo;

(iii) to switch from one to other of the above working conditions in order to maintain stable the rotational speed under the rapid torque fluctuations produced by the air oscillating motion.

The switch function (iii) was experienced to be necessary during a single oscillation cycle of the air column. In fact the flywheel effect had proved to be not-sufficient to maintain nearly constant the rotational speed during the wave period, being friction losses relatively large in respect to the turbine momentum of inertia.

All the actions (i)-(iii) were remotely controlled by a virtual instrument (VI) developed under LABVIEW® environment and running on a personal computer. The VI was interfaced to the power device by a data acquisition board, whose several digital and analog input/outputs were used to drive the turbine.

3 Measurement campaign

We got 261 records, each 5 min long. In every record we obtained four set of variables characterising:

i. the waves in undisturbed field;
ii. the waves in front of the breakwater;
iii. the motion of water and air inside the plant;
iv. the working parameters of the plant and the Wells turbine.

As far as concerns the turbine performance we got the significant height H_s, the peak period T_p, the average angle of the wave direction, the height ζ of the water level inside the chamber, the pressure fluctuations Δp_a in the air pocket. From the measurements of the voltage V_{mot} and the current I_{mot} of the electric DC machine connected to the turbine, and from the rotational speed of the turbine, we obtained the torque produced by the turbine. Through a procedure described in [19], known the mechanical and electrical losses, we determined the internal power P_t produced by the unsteady flow on the blade.

The turbine performance obtained from experiments were converted in the conventional form of non-dimensional coefficient. In details, the measurements of torque are expressed by the torque coefficient T^*:

$$T^* = \frac{T_t}{\rho_a \omega^2 R_{tip}^5}, \tag{1}$$

where T_t is the torque referred to the internal (blade) power P_t

$$T_t = P_t / \omega, \tag{2}$$

ρ_a is the air density, ω is the angular speed, R_{tip} is the blade tip radius; and pressure drop measurements, by the non-dimensional coefficient

$$\Delta p_0^* = \frac{\Delta p_0}{\rho \omega^2 R_{tip}^2}, \tag{3}$$

where Δp_0 is the stagnation pressure drop across the turbine. The characteristic curves are given against the flow coefficient

$$\phi = \frac{V}{\omega R_{tip}}, \tag{4}$$

where V is the average axial velocity in the turbine annulus, evaluated as the ratio between the volumetric flow rate Q and the annulus area A_t:

$$V = \frac{Q}{A_t}. \tag{5}$$

From the measurement of pressure in the central chamber and the total flow rate the (instantaneous) non-dimensional pressure drop as a function of the flow rate has been obtained. A detailed description of the measurement techniques adopted in the experimental campaign is given in [19]. Actually, we measured the pressure drop between the plenum chamber and the atmosphere, neglecting the pressure drop due to minor losses at the air duct ends, and at the turbine hub. Anyhow, the presence of a separator in the connection, curved noses at the inner duct ends, and the outlet guide vane, should have guided, at a certain degree, the flow patterns.

Table 1 – Main data of the examined records.

Record N.	1 H_s [m]	2 T_p [s]	3 n [rpm]	4 ϕ_{rms}	5 Q_{rms} [m^3/s]	6 $\Delta p_{0,rms}$ [Pa]	7 $\frac{\overline{P}_t}{\overline{P}_p}$ %
38	0.320	2.40	1700	0.112	0.135	190.	18.9
54	0.264	6.25	1700	0.164	0.199	340.	21.5
80	0.176	3.55	1700	0.136	0.164	251.	25.8

4 Unsteady Turbine Performance

Here the records of three sea states are examined. The main parameters characterizing the behaviour of the turbine are collected in . They are: the significant wave height H_s, representing the intensity of the incident waves, the peak period of the waves T_p, the rotational speed n, the r.m.s. values of the flow coefficient ϕ_{rms}, the flow rate Q_{rms}, the pressure drop $\Delta p_{0,rms}$ and, finally, the average turbine efficiency,

$\overline{P}_t / \overline{P}_p$ that is obtained as the ratio between the mean turbine power and the pneumatic power. In all the three considered records (no.38, 54, and 80) the rotational speed was set at 1700 rpm.

Record N. 80 is examined first. Figure 3 shows the experimental data of the non-dimensional pressure drop Δp_0^* vs. the flow coefficient ϕ, obtained from a record of 5 minutes at a sampling rate of 10samples/s. Positive values of ϕ represent the flow exiting the chamber towards the atmosphere. Negative values of ϕ represent the entering flow condition: in this condition the pressure drop across the turbine is negative, meaning that the pressure inside the central chamber, which the turbine is connected to, is lower than the atmospheric pressure.

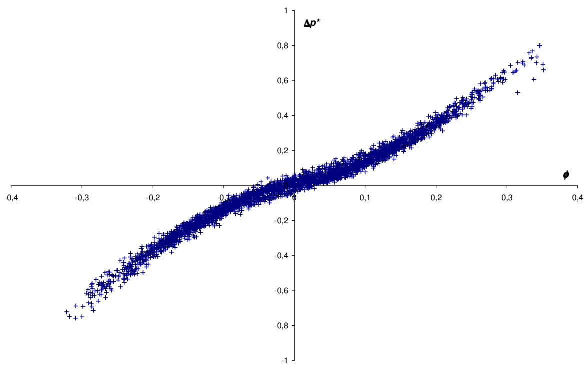

Figure 3 - Non-dimensional pressure drop vs. flow coefficient (record N.80).

It appears that the behaviour is close to be symmetric under inflow and outflow conditions, even if in outflow conditions, the maximum flow rate was about 0.35 higher than the absolute value of 0.32 obtained in the inflow condition. Moreover, the values of the pressure drops appear to be independent of the amplitude of the fluctuations.
From the measurements of the turbine (blade) power, the non-dimensional torque T^* is obtained as a function of the flow coefficient, see Figure 4. It appears that, in outflow condition, the maximum torque coefficient was higher than 0.12 while in inflow condition was always lower than 0.1. The turbine shows also negative torque coefficient with flow coefficient within the range $-0.1 < \phi < 0.1$, due to the drag forces acting on the blades. No stall conditions appear during these records even at the highest values of the absolute value of ϕ.

The instantaneous values of turbine efficiency, evaluated from the ratio between data of pneumatic power and turbine power, are plotted in Figure 5. It appears that the maximum efficiency is about 0.45 that is a value relatively low in comparison with the results given by other authors. This discrepancy is mainly due to the effects of the small dimensions of the turbine and, consequently, low Reynolds Number, as confirmed by steady state measurements and numerical results [14]. It is worth noting that the efficiency does not drop to zero, even with very high values of the flow coefficient. These aspects of the behaviour of the turbine will be discussed later.

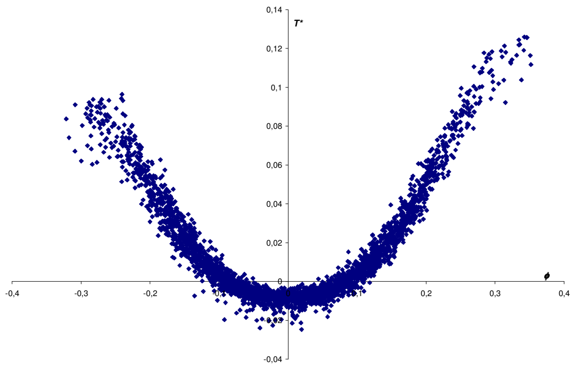

Figure 4 - Non-dimensional blade turbine torque vs. flow coefficient (record N. 80).

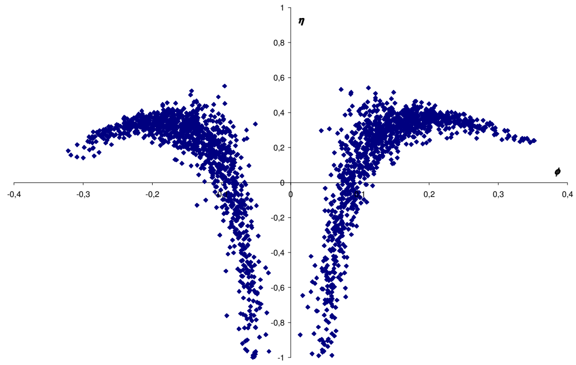

Figure 5 – Blade Turbine efficiency vs. flow coefficient.

5 Regression analysis

As shown in the preceding Section, the measured values of torque coefficient show a certain dispersion, making it difficult to appreciate any signs of hysteresis between the acceleration and deceleration. To this purpose, the curves have been released subject to a process of regression of this kind: from the time history of the flow coefficient ϕ, the derivative $d\phi/dt$ was evaluated; then, the records with $d\phi/dt > 0$ were distinguished from those with $d\phi/dt < 0$. Finally, the range of variation of the flow coefficient ϕ was divided into small intervals with amplitude equal to 0.01. From the values relevant to flow coefficient falling in each interval, two mean values of the torque coefficient were evaluated as a function of ϕ: the first one was the mean value of T^* with $d\phi/dt > 0$, and the second one was the mean of those with $d\phi/dt > 0$.

Figure 6 and Figure 7 show the results of this regression procedure for the non-dimensional pressure drop across the turbine and the torque coefficient, respectively. Comparing the results for outflow ($\phi > 0$) with those relevant to inflow ($\phi < 0$), it appears that the turbine characteristics are about symmetric until the absolute value of the flow coefficient is lower than 0.25. beyond this threshold, the values of the turbine torque become higher for outflow than for inflow conditions. This is most reasonably due to the flow pattern at the inlet of the turbine rotor: as show in Figure 1, the outflow current is better guided by the internal cylindrical wall than the inflow current. This seems not to influence quantitatively the torque until $|\phi|$ is lower than 0.25, while, for higher values of $|\phi|$, it appears that the flow pattern influences the incipient stall condition, starting from values of $|\phi|$ values higher than 0.3.

The asymmetry between inflow and outflow conditions appears to be a peculiarity of OWC systems, due to the asymmetric shape of this kind of plants; shape which makes difficult to have the same flow distribution in the inlet stroke and in the outflow. Also the Limpet plant [28] exhibits a similar asymmetry as a consequence of a non-uniform flow distribution on inlet, resulting from the flow around a resonator plate forming part of the acoustic attenuation system.

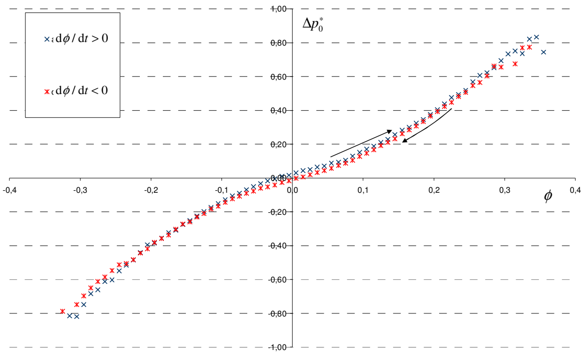

Figure 6 – Regression analysis for the pressure drop coefficient under increasing and decreasing flow coefficient (record N. 80).

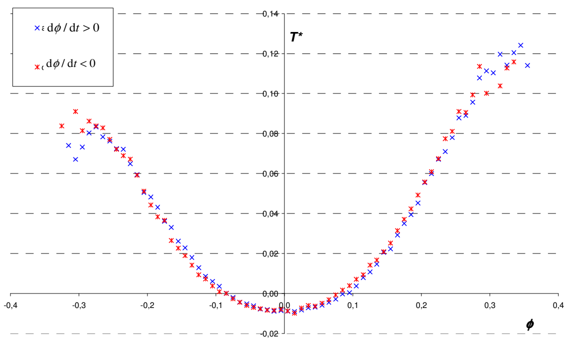

Figure 7 – Comparison of the mean torque coefficient obtained under increasing and decreasing flow coefficient (record N. 80).

6 Influence of flow oscillations on hysteresis

6.1 Frequency effects

In order to investigate about the effects of the frequency on the unsteady behaviour of the turbine, we analysed the power spectrum of the main turbine parameters: pressure drop Δp, flow rate Q, pneumatic power P_p , turbine (blade) power P_t. The power spectra of such quantities, relevant to the sea state record N. 80, are given in Figure 8, where all the plotted quantities are in a non-dimensional form obtained by making the maximum peak equal to 1. It appears that, in the case of sea state N. 80, pressure and flow rate have about the same spectrum, with two peaks close to each other, in the range 0.2-0.25 Hz. The power spectra of pneumatic and turbine power show instead a single peak at a frequency about two times greater, 0.48 Hz. This difference become clear, if we bare in mind that the time needed for one oscillation of the flow rate and pressure drop corresponds to two oscillations of the pneumatic and turbine power.

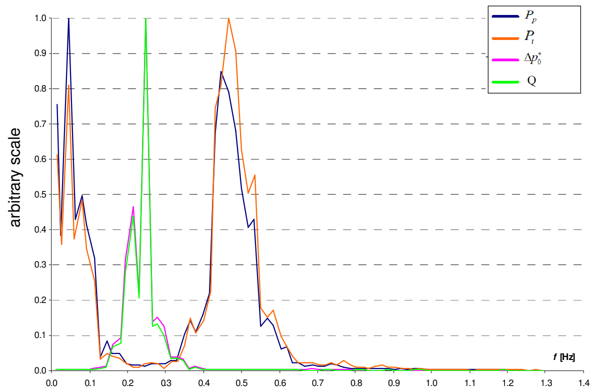

Figure 8 – Power spectrum of pneumatic power, P_p, turbine power P_t, non dimensional pressure drop Δp_0^* and flow rate Q as a function of the frequency f. (record N. 80).

In order to make an analysis of the effects of the frequency on the turbine behaviour, we make a comparison with the results of the sea state record N. 38 (see).

In the record N. 38, Figure 9 and Figure 10 show that the oscillation of the flow coefficient is within the range [-0.3, 0.3], that is about the same observed for record N. 80. The plot of the pressure drop shows also in this case very small differences between the curve relevant to dϕ/dt >0 and with the one relevant to dϕ/dt<0. On the contrary, the results of the torque coefficient shows valuable differences, meaning that, in this case, a hysteretic behaviour of the turbine exists with a counter-clock-wise loop in right side (outflow, $\phi > 0$) and clock-wise loop (about symmetric) in the left side (inflow, $\phi < 0$).

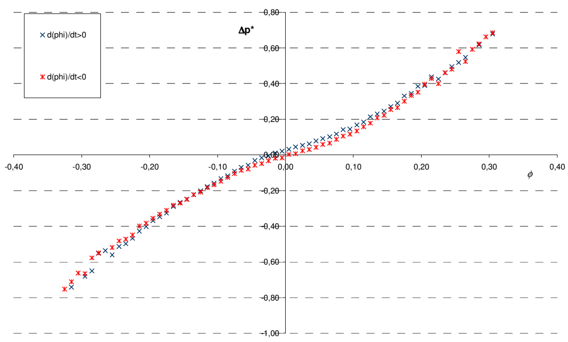

Figure 9 – Regression analysis for the pressure drop coefficient under increasing and decreasing flow coefficient (record N. 38).

From Figure 11, we can observe that both the power spectra of flow rate and pressure drop show two distinct peaks at about 0.2 Hz and 0.5 Hz, while the spectra of pneumatic and turbine power show several peaks. This phenomenon is reasonably due to the higher frequencies observed in this record that caused more rapid rise and decrease of flow rate and, consequently, appreciable differences also at low values of the flow coefficient.

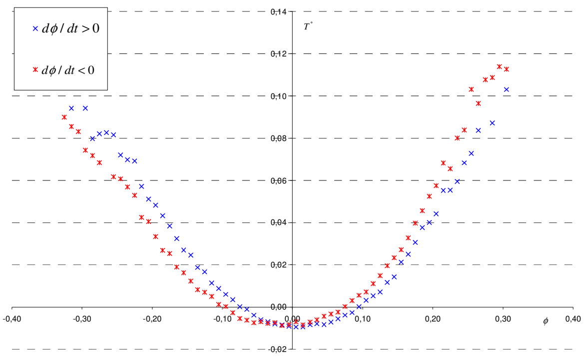

Figure 10 – Comparison of the mean torque coefficient obtained under increasing and decreasing flow coefficient (record N. 38).

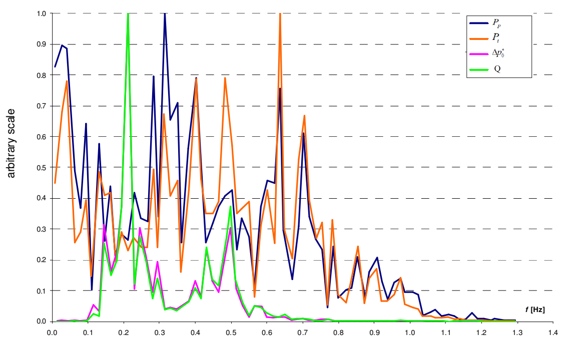

Figure 11 – Power spectrum of pneumatic power, P_p, turbine power P_t, non dimensional pressure drop Δp_0^* and flow rate Q as a function of the frequency f (record N. 38).

<u>6.2 Amplitude effects</u>

In order to investigate on the effects of the amplitude of oscillation of the flow coefficient, we examine the record N. 54, (see). During this record, the oscillation amplitudes of the flow coefficient reached very high values, pushing up to about 0.45 (Figure 12) while the power spectrum (Figure 13) is similar to that of the previously examined record N. 80 (you can see, e.g., a single peak for the pressure drop at about 0.2 Hz). In this case it appears that there is the occurrence of a stall condition, that starts at ϕ about equal to 0.3. When the flow coefficient decreases from 0.45, the torque shows values much lower than those given with increasing flow, until ϕ becomes again lower that 0.3. With further decreasing values of ϕ, the values of torque correspond to the same values showed with increasing flow.

The result of such behaviour is a clockwise hysteretic loop under incipient stall conditions.

The behaviour is qualitatively similar for inflow conditions but the maximum torque obtained under inflow condition is much lower (0.08), mainly due to the non-symmetric geometry of the ducts connected to the turbine, producing different flow patterns depending on the flow direction.

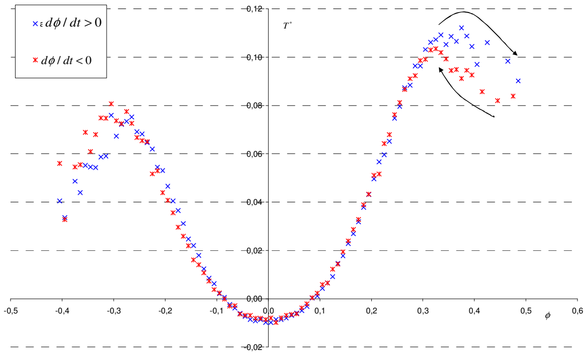

Figure 12 – Comparison of the mean torque coefficient obtained under increasing and decreasing flow coefficient (record N. 54).

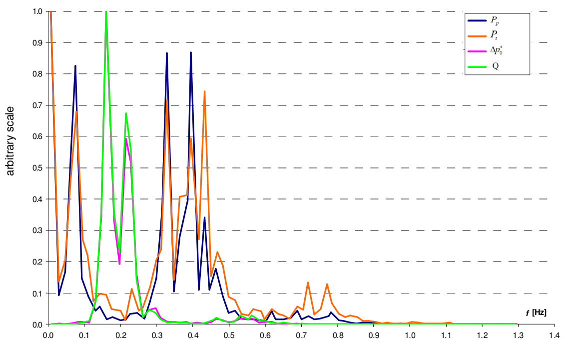

Figure 13 – Power spectrum of pneumatic power, P_p, turbine power P_t, non dimensional pressure drop Δp_0^* and flow rate Q as a function of the frequency f (record N. 54).

7 Conclusions

The paper describes a field experiment on the REWEC3 system equipped with a monoplane Wells turbine without guide vanes.

As far as concerns the turbine unsteady behaviour, results of the experiment can be summarised as follows:

1) the efficiency of conversion of the pneumatic power in turbine (blade) power is about 25% of the pneumatic power due to the small dimensions of the turbine, that lead to low Reynolds number and large influence of secondary losses;
2) the regression analysis made us able to identify appreciable differences concerning inflow and outflow conditions and accelerating and decelerating flows.
3) A first hysteretic mechanism is characterized by a counter-clock-wise (referring to outflow conditions) loop that appears with high frequency oscillations. The amplitude of this loop is little and it concerns mainly the turbine torque.
4) The second hysteretic mechanism is related to the stall conditions and appears with oscillations of very large amplitude, independently from the frequency: after the turbine has fallen in stall, it is unable to reproduce the same torque values

obtained under increasing flow rate, until the flow coefficient becomes lower than a value that can be identified as the flow coefficient of incipient stall conditions.

Acknowledgements

The careful work carried out by the graduated student Graziella Carlo is very appreciated.

References

[1] A. Clément, P. McCullen, A. Falcão, A. Fiorentino, F. Gardner, K. Hammarlund, G. Lemonis, T. Lewis, K. Nielsen, S. Petroncini, M.-T. Pontes, P. Schild, B.-O. Sjöström, H. C. Sørensen, and T. Thorpe. Wave energy in Europe: current status and perspectives. Renewable and Sustainable Energy Reviews, 6:405–431, 2002.

[2] Falcão A. F. de O., 2003 First-generation wave power plant: current status and R&D requirements, Proc. of OMAE2003; 22nd International Conference on Offshore Mechanics and Arctic Engineering, Cancun, Mexico.

[3] S. Raghunathan. TheWells air turbine for wave energy conversion. Prog. Aerosp. Sci., 31:335–386, 1995.

[4] A. Brito-Melo, L. M. C. Gato, and A. J. N. A. Sarmento. Analysis of Wells turbine design parameters by numerical simulation of the OWC performance. Ocean Eng., 29:1463–1477, 2002.

[5] R. Curran, T. P. Stewart, and T. J. T.Whittaker. Design synthesis of oscillating water column wave energy converters: performance matching. Proc. Inst. Mech. Eng., Part A - J. Power Energy, 211:489–505, 1997.

[6] A. Thakker, P. Frawley, and E. Sheik Bajeet. Experimental investigation of CA9 blades on a 0.6 m Wells turbine rig. In 4th European Conference on Turbomachinery, ATI-CST-062/01, Firenze, Italy, 2001.

[7] D. Cocco, F. Nurzia, and P. Puddu. Analisi fluidodinamiche su turbina Wells: risultati sperimentali e teorici ottenuti presso il DIMECA. In III Convegno MiniHydro, Acquafredda di Maratea (PZ), Italy, 2001.

[8] M. Inoue, K. Kaneko, T. Setoguchi, and S. Raghunathan. The fundamental characteristics and future of Wells turbine for wave power generation. Science of Marines, 39:275–280, 1987.

[9] S. Raghunathan, C. P. Tan, and N. A. J. Wells. Theory and performance of a Wells turbine. J. Energy, 6:157–160, 1982.

[10] L. M. C. Gato and A. F. de O. Falc˜ao. On the theory of the Wells turbine. J. Eng. Gas Turbines Power - Trans. ASME, 106:628–633, 1984.

[11] A. Thakker, P. Frawley, and E. S. Bajeet. Performance simulation of CA9 Wells turbine rotor using a 3-D Navier-Stokes explicit solver. In 4th European Conference on Turbomachinery, ATI-CST-063/01, Firenze, Italy, 2001.

[12] T. H. Kim, T. Setoguchi, K. Kaneko, and S. Raghunathan. Numerical investigation on the effect of blade sweep on the performance of Wells turbine. Renew. Energy, 25:235–248, 2002.

[13] T.S. Dhanasekaran and M. Govardhan. Computational analysis of performance and flow investigation on Wells turbine for wave energy conversion. Renew. Energy, 30:2129–2147, 2005.

[14] M. Torresi, S. M. Camporeale, P. D. Strippoli, and G. Pascazio. Accurate numerical simulation of a high solidity Wells turbine. Renew. Energy, 33:735–747, 2008.

[15] Kinoue Y., Setoguchi T., Kim T.H., Kaneko K., Mechanism of Hysteretic Characteristics of Wells Turbine for Wave Power Conversion, Trans. of the ASME, Journal of Fluids Engineering, March 2003, Vol. 125, pp 302-307

[16] Y. Kinoue, T. H. Kim, T. Setoguchi, M. Mohammad, K. Kaneko, and M. Inoue. Hysteretic characteristics ofmonoplane and biplane Wells turbine for wave power conversion. *Energy Conv. Manag.*, 45:1617–1629, 2004.

[17] T. Setoguchi, Y. Kinoue, T. H. Kim, K. Kaneko, andM. Inoue. Hysteretic characteristics Wells turbine for wave power conversion. *Renew. Energy*, 28:2113–2127, 2003.

[18] Thakker A, Abdulhadi R. The performance of Wells turbine under bi-directional airflow. Renew Energy (2008), doi:10.1016/j.renene.2008.02.013

[19] P. Filianoti, S. M. Camporeale, In field measurements on a small scale OWC device, Proceedings of the 8th European Wave and Tidal Energy Conference, Uppsala, Sweden, 2009 (under revision)

[20] Camporeale S. M. and Filianoti P., 2007 A linearized model of OWC devices with additional vertical ducts, 7th European Wave and Tidal Energy Conference (EWTEC), Porto, Portugal

[21] Boccotti P., 2002. US Patent 6450732 B1.

[22] Boccotti P., 2003 On a new wave energy absorber. Ocean Eng. 30, 1191-1200.

[23] Boccotti P., 2003. European Patent EP 1133602 B1

[24] Boccotti P. 2007, European Patent EP 1518052 B1

[25] Boccotti P., 2007 Caisson breakwaters embodying an OWC with a small opening—Part I: Theory, Ocean Engineering 34, 806-819.

[26] Boccotti P., 2007 Comparison between a U-OWC and a conventional OWC", Ocean Engineering 34, 820-841.

[27] Boccotti P., Filianoti P., Fiamma V., Arena F. 2007, Caisson breakwaters embodying an OWC with a small opening—Part II: A small-scale field experiment, Ocean Engineering 34, 820-841.

[28] Wavegen, 2002 Islay Limpet project monitoring final report ETSU V/06/00180/00/Rep.